Displacement of a bubble by acoustic radiation force into a fluid-tissue interface

This is a post-refereeing final draft. When citing, please refer to the published version:

H. Koruk, J.J. Choi, Displacement of a bubble by acoustic radiation force into a fluid–tissue interface, The Journal of the Acoustical Society of America. *143 (4)*, 2535–2540, **2018.**

https://doi.org/10.1121/1.5034175

Displacement of a bubble by acoustic radiation force into a fluid-tissue interface

Hasan Koruk[a)]

Mechanical Engineering Department, MEF University, Istanbul 34396, Turkey

James J. Choi

Noninvasive Surgery and Biopsy Laboratory, Department of Bioengineering, Imperial College London, London SW7 2AZ, United Kingdom

[a)] Author to whom correspondence should be addressed. Electronic mail: korukh@mef.edu.tr

Running title: Bubble into a fluid-tissue interface

Keywords: Bubble; fluid-tissue interface; acoustic radiation force; mathematical model.

ABSTRACT

Microbubbles in an ultrasound beam experience a primary Bjerknes force, which pushes the microbubbles against a fluid-tissue interface and deforms the tissue. This interaction has been used to measure tissue elasticity and is a common interaction in many therapeutic and diagnostic applications, but the mechanisms of deformation, and how the deformation dynamic depends on the bubble and ultrasound parameters, remain unknown. In this study, a mathematical model is proposed for the displacement of a bubble onto a fluid-tissue interface and the tissue deformation in response to the primary Bjerknes force. First, a model was derived for static loading and the model's prediction of bubble-mediated tissue displacement and stresses in tissue were explored. Second, the model was updated for dynamic loading. The results showed that the bubble is both displaced by the applied force and changes its shape. The bubble displacement changes nonlinearly with the applied force. The stress values in tissue are quite high for a distance within one radius of the bubble from the bubble surface. The model proposed here is permissible in human tissue and can be used for biomedical ultrasound applications including material characterization.

PACS numbers: 43.80.Gx, 43.80.Qf, 43.80.Sh

I. INTRODUCTION

Microbubbles in an ultrasound beam experience a primary Bjerknes force, which pushes these microbubbles. There are many studies of bubbles within infinite liquids exposed to a pressure wave in the literature. In fact, several models have been developed for unencapsulated (Keller and Miksis, 1980; Prosperetti, 1987) and encapsulated (Church, 1995; Doinikov et al., 2009; Marmottant et al., 2005) bubbles in a liquid, and for radial oscillations of a bubble in an elastic and viscoelastic medium (Yang and Church, 2005; Zabolotskaya et al., 2005; Barajas and Johnsen, 2017). Mathematical models for the displacement of a bubble embedded in a tissue have also been proposed (Ilinskii et al., 2005). But bubbles are often present along fluid-tissue interfaces during ultrasound imaging (Erpelding et al., 2005) (Doherty et al., 2013) and therapeutic applications (Haar, 2007). In these situations, it would be useful to be able to predict the deformation and stress applied to the tissue for different ultrasound and microbubble parameters.

Techniques, based on the application of ultrasound and monitoring of the deformation or force response, have been used in practice to determine tissue properties such as the elasticity modulus (Ophir et al., 1991; Fatemi and Greenleaf, 1998; Nightingale et al., 2001). The use of microbubbles, where bubbles push tissue under ultrasound exposure, was proposed to improve the contrast and spatial resolution of elasticity imaging (Koruk et al., 2015). However, the mechanisms of deformation, and how the deformation dynamic depends on the bubble and ultrasound parameters, remain unknown. It should be noted that a bubble pushed by ultrasound has been previously used for tissue characterization by using mathematical models for a particle embedded in a tissue (Ilinskii et al., 2005; Chen et al., 2002; Aglyamov et al., 2007; Karpiouk et al., 2009; Urban et al., 2011; Yoon et al., 2011). This technique uses a high-powered laser to generate the bubble. Therefore, this limits its application to shallow targets and requires local destruction of the material. Thus, the technique based on bubble

generation using laser induced optical breakdown in the medium may not be permissible in human tissue. Furthermore, microbubbles and other contrast agents are not embedded in tissue in practice instead they are administered in blood.

In this study, a mathematical model is proposed for the displacement of a bubble onto a fluid-tissue interface and the tissue deformation in response to the primary Bjerknes force. The technique used here is based on the approach used for the displacement of a spherical object embedded in a bulk material (Ilinskii et al., 2005; Landau and E. M. Lifshitz, 1987). First, a model was derived for static loading and the model's prediction of bubble-mediated tissue displacement and stresses in tissue were explored. Second, the model was updated for dynamic loading. The results showed that the model is capable of predicting the bubble displacement in fluid-tissue interface and tissue deformation, thus can be used for biomedical ultrasound applications including the design of experiments and material characterization.

II. MATHEMATICAL MODEL

A bubble moves in fluid (Fig. 1a) and then displaces tissue when it is exposed to an acoustic radiation force (Fig. 1b). The problem here is axisymmetric, hence the deformation is symmetric along the axial (x) direction and the vector of displacement due to an acoustic radiation force f_e has radial (u_r) and polar (u_θ) components.

(a) **(b)**

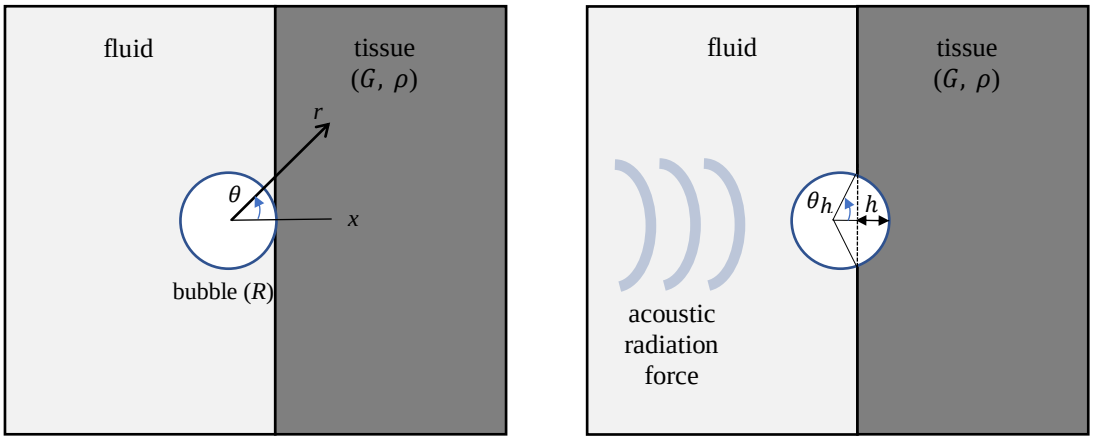

FIG. 1. (Color online) (a) A bubble with a radius of *R* moves in fluid and then (b) displaces tissue with a shear modulus *G* and density ρ when it is exposed to an acoustic radiation force.

A. Static loading

Most tissues can be considered incompressible (Sarvazyan, 1975). Assuming the medium is elastic, isotropic, homogeneous, incompressible and inviscous, the displacement vector can be written as (Ilinskii et al., 2005):

$$\mathbf{u} = \boldsymbol{\nabla} \mathrm{x} \boldsymbol{\nabla} (g\mathbf{e}) \tag{1}$$

where $\mathbf{e}$ is a unit vector along the displacement vector and $g = g(r)$ is a scalar function given by:

$$g(r) = ar + \frac{b}{r} \tag{2}$$

Here a and b are constants determined by using boundary conditions on the object surface and r is the radial coordinate. When the polar axis of the spherical system of coordinates is along the displacement vector, the components of displacement vector are given by:

$$u_r = \frac{2}{r^2}\left(-ar + \frac{b}{r}\right)\cos\theta \tag{3a}$$

$$u_\theta = \frac{1}{r}\left(a + \frac{b}{r^2}\right)\sin\theta \tag{3b}$$

where θ is angle between the radial coordinate (r) and axial (x) direction as depicted in Fig. 1. The pressure in the medium is given by:

$$p = p_0 + G(\mathbf{e} \cdot \boldsymbol{\nabla})\nabla^2 g \tag{4}$$

where p_0 is the pressure far away from the object and G is the shear modulus of material. It should be noted that the elasticity modulus is related to the shear modulus by $E = 2G(1 + \nu)$ for homogeneous isotropic materials where ν is Poisson's ratio. The force on a displaced spherical object in elastic medium is given by (Landau and E. M. Lifshitz, 1987):

$$f = \int(-p\cos\theta + \sigma_{rr}\cos\theta - \sigma_{r\theta}\sin\theta)\,\mathrm{d}S \tag{5}$$

where σ_{rr} and $\sigma_{r\theta}$ are stress tensor components and $\mathrm{d}S$ is an element of spherical surface. For the problem illustrated in Fig. 1, Eq. (5) can be written as:

$$f = \int_0^{\theta_h}(-p\cos\theta + \sigma_{rr}\cos\theta - \sigma_{r\theta}\sin\theta)2\pi R\sin\theta R\mathrm{d}\theta \tag{6a}$$

or

$$f = 2\pi R^2 \int_0^{\theta_h}(-p\cos\theta + \sigma_{rr}\cos\theta - \sigma_{r\theta}\sin\theta)\sin\theta\mathrm{d}\theta \tag{6b}$$

where θ_h is the angle corresponding to the displacement h. The components of stress tensor within a spherical system of coordinates become:

$$\sigma_{rr} = 2G\frac{\partial u_r}{\partial r} = 4G\left(\frac{a}{r^2} - \frac{3b}{r^4}\right)\cos\theta \tag{7a}$$

$$\sigma_{r\theta} = G\left(\frac{\partial u_\theta}{\partial r} - \frac{u_\theta}{r} + \frac{1}{r}\frac{\partial u_r}{\partial \theta}\right) = -\frac{6G}{r^4}b\sin\theta \tag{7b}$$

The boundary condition at the bubble surface (i.e., at $r = R$) is $\sigma_{r\theta} = 0$ and this gives $b = 0$. Thus, the expressions displacement vector components, the radial component of stress tensor σ_{rr} and pressure are reduced to:

$$u_r = -\frac{2a}{r}\cos\theta \tag{8a}$$

$$u_\theta = \frac{a}{r}\sin\theta \tag{8b}$$

$$\sigma_{rr} = \frac{4Ga}{r^2}\cos\theta \tag{9}$$

$$p = p_0 - \frac{2Ga}{r^2}\cos\theta \tag{10}$$

The value of a is estimated using the equilibrium equation stating that the pressure outside the object including the pressure in the medium p, the normal stress σ_{rr} acting on the object, and the acoustic radiation pressure p_e is balanced by the internal pressure in the object p_g:

$$p - \sigma_{rr} + p_e = p_g \tag{11}$$

The radiation pressure p_e here is the external force per unit area acting on the bubble surface. Since the radiation force changes with θ, the pressure p_e is also as a function of θ:

$$p_\mathrm{e} = p_{\mathrm{e}0}\cos\theta \tag{12}$$

where $p_{\mathrm{e}0}$ is the pressure for $\theta = 0$, and its value is defined by the equation for the radiation force:

$$f_\mathrm{e} = 2\pi R^2 \int_0^{\theta_h} (-p_\mathrm{e}\cos\theta)\sin\theta \mathrm{d}\theta \tag{13}$$

Substitution of Eq. (12) into Eq. (13) and integration yields:

$$p_{\mathrm{e}0} = \frac{3f_\mathrm{e}}{2\pi R^2(\cos^3\theta_h - 1)} \tag{14}$$

Substitution of Eqs. (9), (10), (12) and (14) into Eq. (11) and setting $r = R$ and $p_g = p_0$ yields:

$$a = \frac{f_\mathrm{e}}{4\pi G\left(\left(1-\frac{u_{r0}}{R}\right)^3 - 1\right)} \tag{15}$$

where u_{r0} is the radial stress component for $\theta = 0$. Thus, the displacement components and the radial stress component then become:

$$u_r = \frac{f_\mathrm{e}}{2\pi Gr\left[1-\left(1-\frac{u_{r0}}{R}\right)^3\right]}\cos\theta \tag{16a}$$

$$u_\theta = -\frac{f_\mathrm{e}}{4\pi Gr\left[1-\left(1-\frac{u_{r0}}{R}\right)^3\right]}\sin\theta \tag{16b}$$

$$\sigma_{rr} = -\frac{f_\mathrm{e}}{\pi r^2\left[1-\left(1-\frac{u_{r0}}{R}\right)^3\right]}\cos\theta \tag{17}$$

It should be noted that the impedance mismatch between the bubble and the surrounding fluid or tissue is far greater than the mismatch between the fluid and tissue. As a result, we have ignored the deformation of the fluid-tissue interface. The model can be used to predict displacement of large and small bubbles. However, the surface tension effect, which was not included here, is significant for small bubbles and specifically for bubble shape changes. The inclusion of surface tension into the model will be considered in a future study.

B. Dynamic Loading

Here, we investigate the displacement of a gas bubble in an elastic incompressible medium when the external force depends on time. The displacement of the bubble will be as in Eq. (1). However, this time the function $g(r)$ is defined as (Ilinskii et al., 2005):

$$g(r) = \frac{\tilde{a}\mathbf{e}^{jkr}}{jkr} - \frac{\tilde{b}}{r} \tag{18}$$

where $\tilde{a}$ and $\tilde{b}$ are complex constants determined by using boundary conditions, while k is a wave number for a shear wave of frequency ω given by:

$$k^2 = \frac{\omega^2}{c_t^2} = \frac{\rho\omega^2}{G} \tag{19}$$

The components of displacement vector in this case are given by:

$$U_r = -\frac{2}{r^2}\left[\tilde{a}\mathbf{e}^{jkr}\left(1 - \frac{1}{jkr}\right) + \frac{\tilde{b}}{r}\right]\cos\theta \tag{20a}$$

$$U_\theta = -\frac{1}{r^2}\left[\tilde{a}\mathbf{e}^{jkr}\left(1 - jkr - \frac{1}{jkr}\right) + \frac{\tilde{b}}{r}\right]\sin\theta \tag{20b}$$

The pressure equation is:

$$p = p_0 + G(\mathbf{e}\cdot\boldsymbol{\nabla})(\nabla^2 g + k^2 g) \tag{21}$$

where p_0 is the pressure far away from the object. Using the boundary condition at the bubble surface (i.e., at $r = R$) being $\sigma_{r\theta} = 0$ and Eq. (20), we have:

$$\sigma_{r\theta} = -\frac{G}{R^3}\left[\tilde{a}\mathbf{e}^{jkR}\left(3jkR + k^2R^2 - 6 + \frac{6}{jkR}\right) - \frac{6\tilde{b}}{r}\right]\sin\theta = 0 \tag{22}$$

Here $\tilde{b}$ is determined to be:

$$\tilde{b} = \tilde{a}\mathbf{e}^{jkR}R\left(\frac{1}{2}jkR + \frac{1}{6}k^2R^2 - 1 + \frac{1}{jkR}\right) \tag{23}$$

So, the expressions of the displacement vector components are reduced to:

$$U_r = U_\omega\left(1 - \frac{1}{3}jkR\right)\cos\theta \tag{24a}$$

$$U_\theta = -\frac{U_\omega}{2}\left(1 + \frac{1}{3}jkR\right)\sin\theta \tag{24b}$$

Here U_ω is given by:

$$U_\omega = -\frac{ik}{R}\tilde{a}\mathbf{e}^{jkR} \tag{24c}$$

and is interpreted as low-frequency displacement. The radial component of stress tensor σ_{rr} at the bubble surface, and the pressure in the medium around the moving bubble are reduced to:

$$\sigma_{rr} = -\frac{2G}{R}U_\omega(1 - jkR)\cos\theta \tag{25}$$

$$p = p_0 + \frac{G}{R}U_\omega\left(1 - jkR - \frac{1}{2}k^2R^2 + \frac{1}{6}jk^3R^3\right)\cos\theta \tag{26}$$

Performing operations similar to the static case expression describing bubble displacement induced by external force $F_{e\omega}$ is obtained as:

$$F_{e\omega} = 2\pi GRU_\omega(1 - \cos^3\theta_h)\left(1 - jkR - \frac{1}{6}k^2R^2 + \frac{1}{18}jk^3R^3\right) \tag{27}$$

In the time domain, the equation for the bubble oscillations looks like:

$$\underline{u} + \dot{\underline{u}} + \frac{1}{6}\ddot{\underline{u}} + \frac{1}{18}\dddot{\underline{u}} = \underline{f_e} \tag{28}$$

Equation (28) is written by dimensionless displacement, external force and time, given by:

$$\underline{u} = \frac{u(t)}{R} \tag{29a}$$

$$\underline{f_e} = \frac{f_e}{2\pi GR^2(1-\cos^3\theta_h)} \tag{29b}$$

$$\underline{t} = \frac{t\sqrt{G/\rho}}{R} \tag{29c}$$

The solution of Eq. (28) will provide the dynamic force-displacement relation for a bubble onto a fluid-tissue interface.

The model presented here can be improved for more accurate displacement predictions. Although the radial and translational bubble oscillatory motion can be kept small when proper excitation parameters are selected (Watanabe and Kukita, 1993; Zheng et al., 2007; Mettin and Doinikov, 2009), the use of different bubble models including radial and translational oscillatory bubble dynamics will be considered in future studies.

III. RESULTS AND DISCUSSION

Here analyses are performed for physiologically relevant material properties (e.g., G = 0.5 – 4 kPa and $\rho = 1000$ kg/m^3) and bubble radii (R = 1 – 5 μm) mostly encountered in practice (Koruk et al., 2015). The dimensionless force $f_e/(u_{r0}GR)$ changes from zero to 4π as the dimensionless displacement u_{r0}/R increases from zero to two for a bubble onto a fluid-tissue interface (Fig. 2a). It should be noted that the dimensionless force does not change with the dimensionless displacement for a bubble embedded in a bulk material. The bubble displacement increases linearly with the applied force for the embedded bubble. However, the displacement-force relation is nonlinear for a bubble onto a fluid-tissue interface (Fig. 2b). It is seen that u_{r0}/R changes from 0 to 0.5 as force increases from 0 to 70 nN for physiological relevant parameters (e.g., G = 1 kPa, R = 1 - 5 μm). Thus, force is selected between 0 and 70 nN for the subsequent analyses.

(a) **(b)**

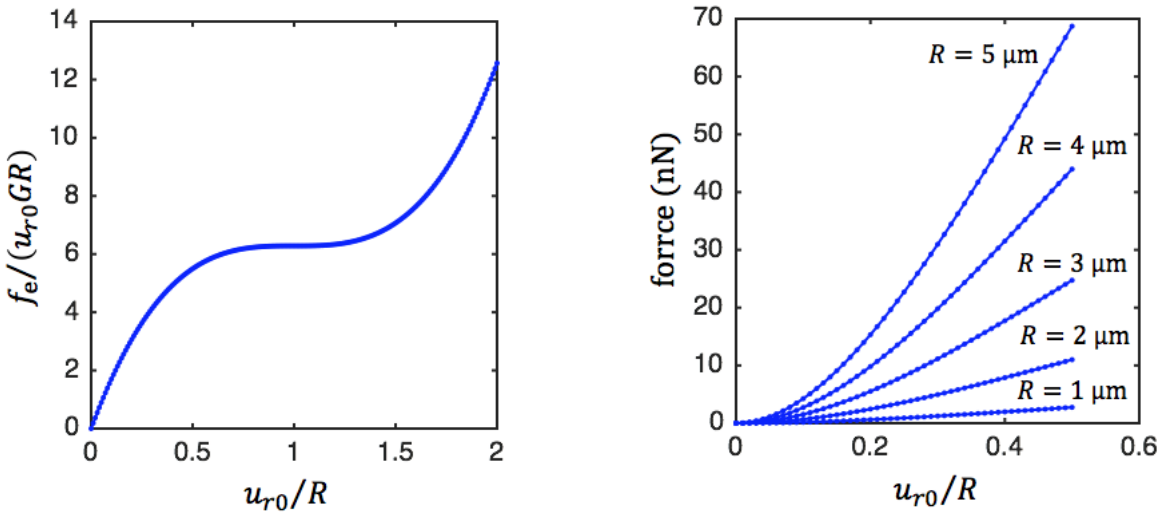

FIG. 2. (Color online) (a) The dimensionless force $f_e/(u_{r0}GR)$ and (b) displacement-force relation for a bubble onto a fluid-tissue interface for different bubble radii (shear modulus is $G = 1$ kPa here).

Results show that a bubble onto a fluid-material interface is both displaced by the applied force and also changes its shape (Fig. 3). The bubble remains almost spherical for forces producing a displacement of up to half the bubble radius. It is seen that the maximum displacement and stress in material are around 1 μm and 0.5 kPa, respectively, for a typical bubble radius (2 μm) encountered in practice and a force amplitude of 10 nN (Fig. 4). Results show that the stress values are high for a distance within one radius of the bubble from the bubble surface, while the values are quite low in the region where the distance from the bubble surface is greater than two radii (Fig. 4).

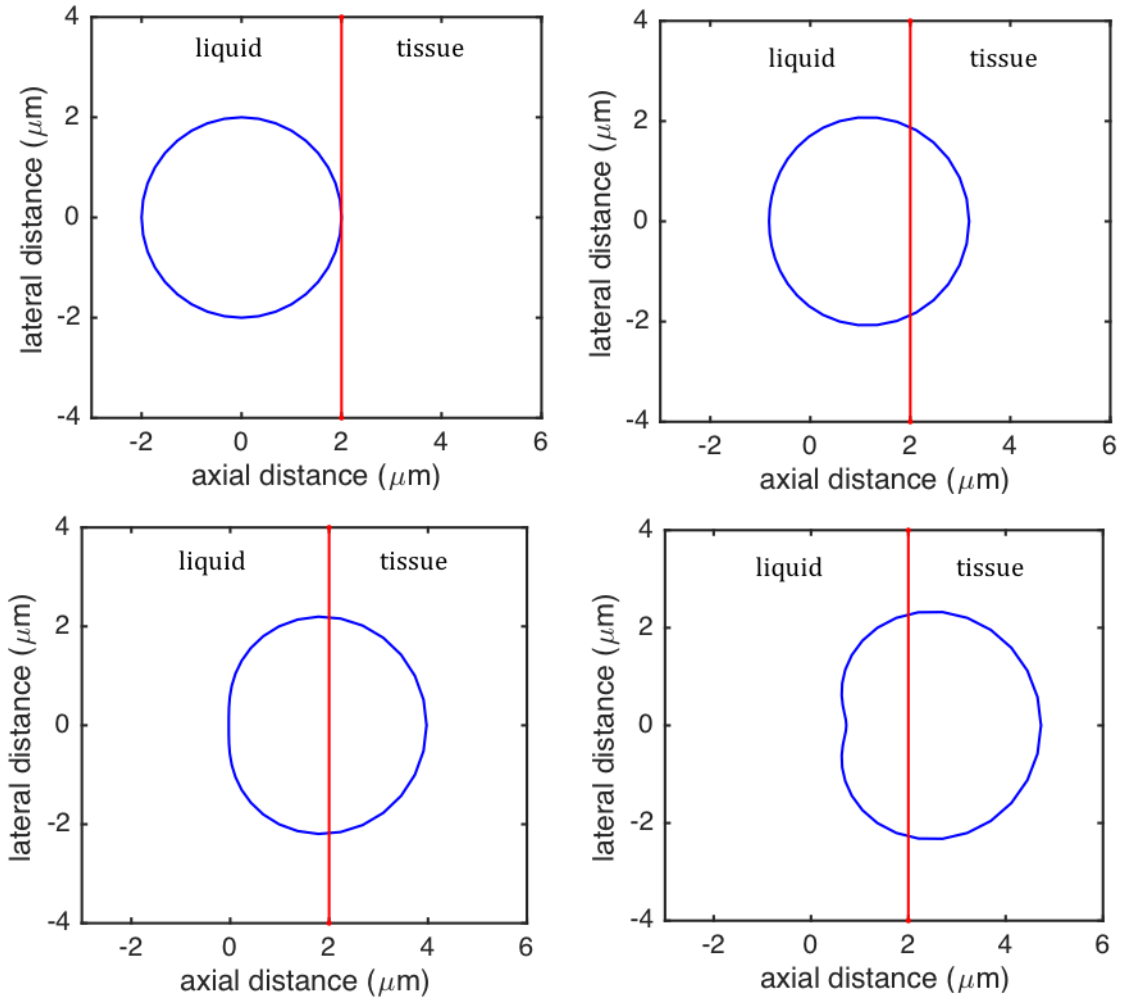

FIG. 3. (Color online) Bubble displacement for a bubble radius $R = 2$ μm, shear modulus $G = 1$ kPa and different force values (0, 10, 20 and 30 nN).

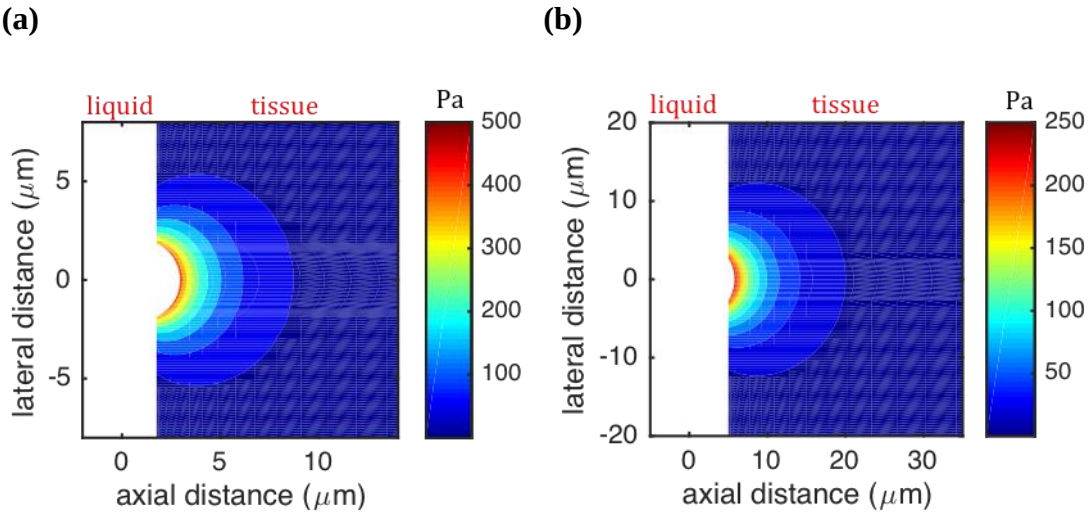

FIG. 4. (Color online) Stress distribution for a bubble radius (a) $R = 2$ and (b) 5 μm (shear modulus is $G = 1$ kPa and force is 10 nN here).

Equation (28) is solved for an impulsive force with an amplitude $\underline{f_e}$ and a duration $\underline{\tau}$ where small and large $\underline{\tau}$ values correspond to short and long pulses, respectively. The normalized dimensionless impulsive response $\underline{u}_{r0}/(R\underline{f_e})$ for different duration $\underline{\tau}$ values presented as a function of dimensionless time $\underline{t}$ in Fig. 5 shows that the response resembles the unit impulse response and step response as the duration $\underline{\tau}$ takes small and large values, respectively. It can be seen that the displacement reaches an almost steady-state value of around $\underline{t} = 5$. It is worth noting that the pulse length required for a steady-state displacement in experiments in practice can be calculated using this value and Eq. (29c). It is clear that softer materials will take longer time to reach to the steady state.

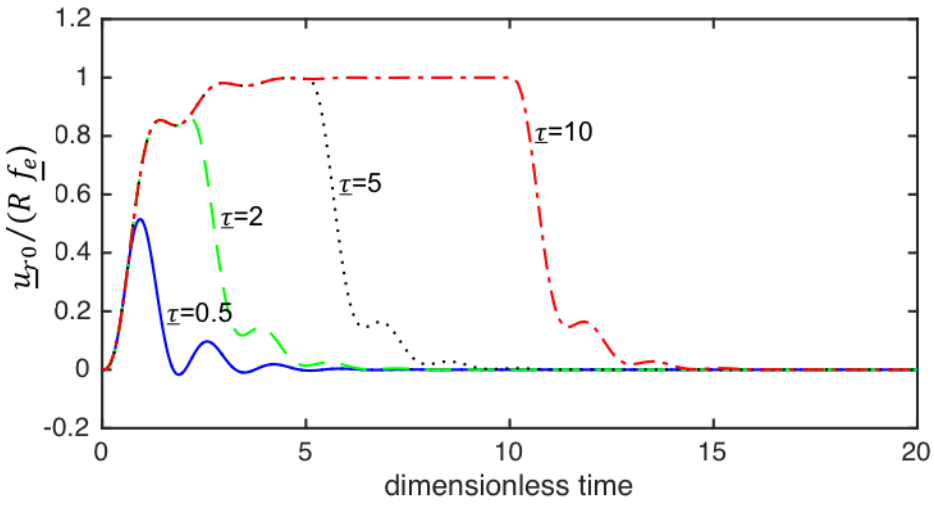

FIG. 5. (Color online) The normalized dimensionless impulsive response $\underline{u}_{r0}/(R\underline{f}_e)$ for an amplitude $\underline{f}_e$ and different duration $\underline{\tau}$ values as a function of the dimensionless time $\underline{t}$.

The impulsive response for $R = 2$ μm, $\rho = 1000$ kg/m^3, $G = 1$ kPa, $\tau = 10$ μs and different force amplitude (A) values as a function of time in Fig. 6 shows that displacement increases as force increases as expected. The steady-state amplitude changes nonlinearly with the applied force. It should be noted that the model can be used to design bubbles (e.g., radius) and pulses (e.g., pulse length and amplitude). Furthermore, it can be used to predict the order of possible displacements for a specific input and thus determine the resolution of the equipment (e.g., microscope) required in experiments in practice when material properties are known approximately.

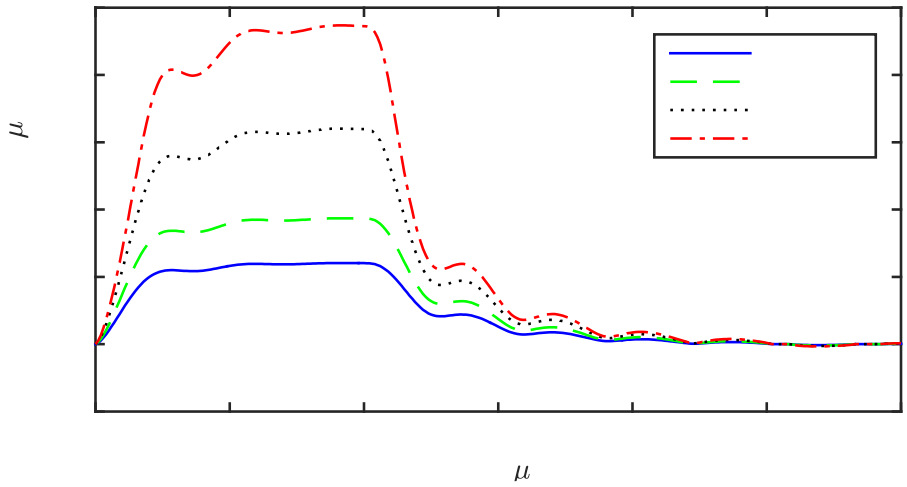

FIG. 6. (Color online) The impulsive response for $R = 2$ μm, $G = 1$ kPa, $\rho = 1000$ kg/m^3, $\tau = 10$ μs and different force amplitude (A) values.

The impulsive response for $R = 2$ μm, $\rho = 1000$ kg/m^3, $f_e = 10$ nN, $\underline{\tau} = 5$ and different shear modulus (G) values as a function of time in Fig. 7 shows that the displacement and the time required for the steady-state response decreases as shear modulus increases. In fact, τ values corresponding to $\underline{\tau}$ = 5 are 14.1, 10.0, 7.1, and 5.0 μs for $G = 0.5$, 1, 2 and 4 kPa, respectively. The period of oscillations decreases as the shear modulus value increases.

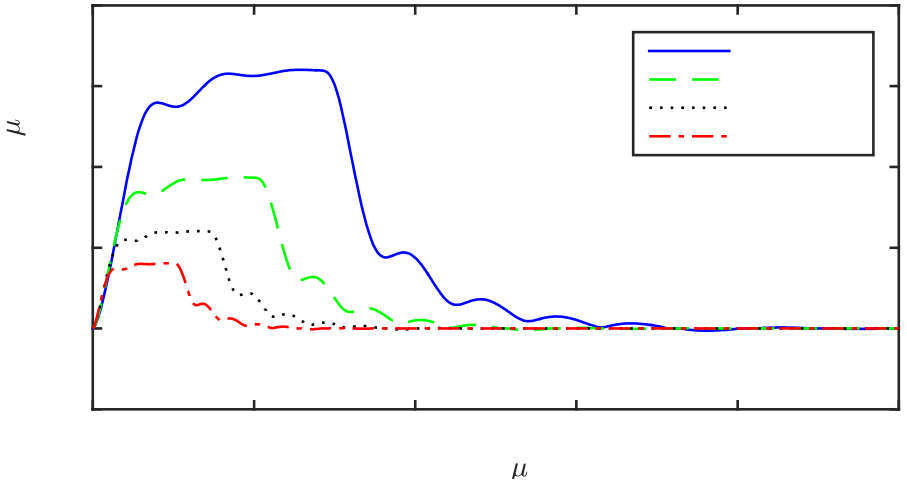

FIG. 7. (Color online) The impulsive response for $R = 2$ μm, $\rho = 1000$ kg/m^3, $f_e = 10$ nN, $\underline{\tau}$ = 5 and different shear modulus (G) values.

The model presented here seems appropriate to be used to predict the amount of deformation and stresses in materials in biomedical ultrasound applications. The model presented here is of practical importance and can be used for biomedical ultrasound applications including the design of experiments and material characterization.

IV. CONCLUSION

In this study, a mathematical model was proposed for the displacement of a bubble onto a fluid-tissue interface and the tissue deformation in response to the primary Bjerknes force. First, a model was derived for static loading and the model's prediction of bubble-mediated tissue displacement and stresses in tissue were explored. Second, the model was updated for dynamic loading. The results show that bubble displacement changes nonlinearly with the applied force for a bubble onto a fluid-tissue interface. The bubble is both displaced by the applied force and changes its shape. The bubble remains almost spherical for a force producing a displacement which is less than the bubble radius. The stress values in the tissue around the bubble for a region within a distance of a radius from the bubble surface are high, while the stress values are quite low when the distance is greater than two radii. For dynamic loading, the increase in steady-state amplitude changes nonlinearly with the applied force. The time required for steady-state response decreases as the shear modulus increases. It is seen that the proposed model is capable of predicting the bubble displacement onto a fluid-tissue interface and tissue deformation and, thus, can be used in biomedical ultrasound applications including the design of experiments and material characterization.

REFERENCES

Aglyamov, S. R., Karpiouk, A. B., Ilinskii, Y. A., Zabolotskaya, E. A., and Emelianov, S. Y. (**2007**). "Motion of a solid sphere in a viscoelastic medium in response to applied acoustic radiation force: Theoretical analysis and experimental verification," J. Acoust. Soc. Am., **122**, 1927–1936. doi:10.1121/1.2774754

Barajas, C., and Johnsen, E. (**2017**). "The effects of heat and mass diffusion on freely oscillating bubbles in a viscoelastic, tissue-like medium," J. Acoust. Soc. Am., **141**, 908–918. doi:10.1121/1.4976081

Chen, S., Fatemi, M., and Greenleaf, J. F. (**2002**). "Remote measurement of material properties from radiation force induced vibration of an embedded sphere," J. Acoust. Soc. Am., **112**, 884–889. doi:10.1121/1.1501276

Church, C. C. (**1995**). "The effects of an elastic solid surface layer on the radial pulsations of gas bubbles," J. Acoust. Soc. Am., **97**, 1510–1521. doi:10.1121/1.412091

Doherty, J., Trahey, G., Nightingale, K., and Palmeri, M. (**2013**). "Acoustic Radiation Force Elasticity Imaging in Diagnostic Ultrasound," IEEE Trans. Ultrason. Ferroelectr. Freq. Control, **60**, 685–701. doi:10.1109/TUFFC.2013.2617

Doinikov, A. A., Haac, J. F., and Dayton, P. A. (**2009**). "Modeling of nonlinear viscous stress in encapsulating shells of lipid-coated contrast agent microbubbles," Ultrasonics, **49**, 269–275. doi:10.1016/J.ULTRAS.2008.09.007

Erpelding, T. N., Hollman, K. W., and O'Donnell, M. (**2005**). "Bubble-based acoustic radiation force elasticity imaging," Ultrason. Ferroelectr. Freq. Control. IEEE Trans., **52**, 971–979. doi:10.1109/TUFFC.2005.1504019

Fatemi, M., and Greenleaf, J. F. (**1998**). "Ultrasound-Stimulated Vibro-Acoustic Spectrography," Science (80-.)., **280**, 82 LP-85. Retrieved from http://science.sciencemag.org/content/280/5360/82.abstract

Haar, G. ter (**2007**). "Therapeutic applications of ultrasound," Prog. Biophys. Mol. Biol., **93**, 111–129. doi:10.1016/J.PBIOMOLBIO.2006.07.005

Ilinskii, Y. A., Meegan, G. D., Zabolotskaya, E. A., and Emelianov, S. Y. (**2005**). "Gas bubble and solid sphere motion in elastic media in response to acoustic radiation force," J. Acoust. Soc. Am., **117**, 2338–2346. doi:10.1121/1.1863672

Karpiouk, A. B., Aglyamov, S. R., Ilinskii, Y. A., Zabolotskaya, E. A., and Emelianov, S. Y. (**2009**). "Assessment of shear modulus of tissue using ultrasound radiation force acting on a spherical acoustic inhomogeneity," IEEE Trans. Ultrason. Ferroelectr. Freq. Control, **56**, 2380–2387.

Keller, J. B., and Miksis, M. (**1980**). "Bubble oscillations of large amplitude," J. Acoust. Soc. Am., **68**, 628–633. doi:10.1121/1.384720

Koruk, H., El Ghamrawy, A., Pouliopoulos, A. N., and Choi, J. J. (**2015**). "Acoustic particle palpation for measuring tissue elasticity," Appl. Phys. Lett., **107**, 223701. doi:10.1063/1.4936345

Landau, L. D., and E. M. Lifshitz (**1987**). *Fluid Mechanics*, Pergamon, New York, 2nd ed.

Marmottant, P., van der Meer, S., Emmer, M., Versluis, M., de Jong, N., Hilgenfeldt, S., and Lohse, D. (**2005**). "A model for large amplitude oscillations of coated bubbles accounting for buckling and rupture," J. Acoust. Soc. Am., **118**, 3499–3505. doi:10.1121/1.2109427

Mettin, R., and Doinikov, A. A. (**2009**). "Translational instability of a spherical bubble in a standing ultrasound wave," Appl. Acoust., **70**, 1330–1339. doi:https://doi.org/10.1016/j.apacoust.2008.09.016

Nightingale, K. R., Palmeri, M. L., Nightingale, R. W., and Trahey, G. E. (**2001**). "On the feasibility of remote palpation using acoustic radiation force," J. Acoust. Soc. Am., **110**, 625–634. doi:10.1121/1.1378344

Ophir, J., Céspedes, I., Ponnekanti, H., Yazdi, Y., and Li, X. (**1991**). "Elastography: A Quantitative Method for Imaging the Elasticity of Biological Tissues," Ultrason. Imaging, **13**, 111–134. doi:10.1177/016173469101300201

Prosperetti, A. (**1987**). "The equation of bubble dynamics in a compressible liquid," Phys. Fluids, **30**, 3626–3628. doi:10.1063/1.866445

Sarvazyan, A. P. (**1975**). "Low-frequency acoustic characteristics of biological tissues," Polym. Mech., **11**, 594–597. doi:10.1007/BF00856791

Urban, M. W., Nenadic, I. Z., Mitchell, S. A., Chen, S., and Greenleaf, J. F. (**2011**). "Generalized response of a sphere embedded in a viscoelastic medium excited by an ultrasonic radiation force," J. Acoust. Soc. Am., **130**, 1133–1141. doi:10.1121/1.3613939

Watanabe, T., and Kukita, Y. (**1993**). "Translational and radial motions of a bubble in an acoustic standing wave field," Phys. Fluids A Fluid Dyn., **5**, 2682–2688. doi:10.1063/1.858731

Yang, X., and Church, C. C. (**2005**). "A model for the dynamics of gas bubbles in soft tissue," J. Acoust. Soc. Am., **118**, 3595–3606. doi:10.1121/1.2118307

Yoon, S., Aglyamov, S. R., Karpiouk, A. B., Kim, S., and Emelianov, S. Y. (**2011**).

"Estimation of mechanical properties of a viscoelastic medium using a laser-induced microbubble interrogated by an acoustic radiation force," J. Acoust. Soc. Am., **130**, 2241–2248. doi:10.1121/1.3628344

Zabolotskaya, E. A., Ilinskii, Y. A., Meegan, G. D., and Hamilton, M. F. (**2005**). "Modifications of the equation for gas bubble dynamics in a soft elastic medium," J. Acoust. Soc. Am., **118**, 2173–2181. doi:10.1121/1.2010348

Zheng, H., Dayton, P. A., Caskey, C., Zhao, S., Qin, S., and Ferrara, K. W. (**2007**). "Ultrasound-Driven Microbubble Oscillation and Translation Within Small Phantom Vessels," Ultrasound Med. Biol., **33**, 1978–1987. doi:https://doi.org/10.1016/j.ultrasmedbio.2007.06.007